Comparison of Ventilated and Unventilated Air Temperature Measurements in Inland Dronning Maud Land on the East Antarctic Plateau

SHOHEI MORINO,[a] NAOYUKI KURITA,[a,b] NAOHIKO HIRASAWA,[c] HIDEAKI MOTOYAMA,[c] KONOSUKE SUGIURA,[d] MATTHEW LAZZARA,[e,f] DAVID MIKOLAJCZYK,[e,g] LEE WELHOUSE,[e,f] LINDA KELLER,[e,g] AND GEORGE WEIDNER[e,g]

[a] *Graduate School of Environmental Studies, Nagoya University, Nagoya, Japan*
[b] *Institute of Space-Earth Environmental Science, Nagoya University, Nagoya, Japan*
[c] *National Institute of Polar Research, Tokyo, Japan*
[d] *Department of Earth System Science, School of Sustainable Design, University of Toyama, Toyama, Japan*
[e] *Antarctic Meteorological Research and Data Center, Space Science and Engineering Center, University of Wisconsin–Madison, Madison, Wisconsin*
[f] *Department of Physical Sciences, School of Engineering, Science and Mathematics, Madison Area Technical College, Madison, Wisconsin*
[g] *Department of Atmospheric and Oceanic Science, University of Wisconsin–Madison, Madison, Wisconsin*

(Manuscript received 27 July 2021, in final form 13 October 2021)

ABSTRACT: Surface temperature measurements with naturally ventilated (NV) sensors over the Antarctic Plateau are largely subject to systematic errors caused by solar radiative heating. Here we examined the radiative heating error in Dronning Maud Land on the East Antarctic Plateau using both the newly installed automatic weather stations (AWSs) at NDF and Relay Station and the existing AWSs at Relay Station and Dome Fuji. Two types of NV shields were used in these AWSs: a multiplate radiation shield and a simple cylinder-shaped shield. In austral summer, the temperature bias between the force-ventilated (FV) sensor and the NV sensor never reached zero because of continuous sunlight. The hourly mean temperature errors reached up to 8°C at noon on a sunny day with weak wind conditions. The errors increased linearly with increasing reflected shortwave radiation and decreased nonlinearly with increasing wind speed. These features were observed in both the multiplate and the cylinder-shaped shields. The magnitude of the errors of the multiplate shield was much larger than that of the cylinder-shaped shield. To quantify the radiative errors, we applied an existing correction model based on the regression approach and successfully reduced the errors by more than 70% after the correction. This indicates that we can use the corrected temperature data instead of quality controlled data, which removed warm bias during weak winds in inland Dronning Maud Land.

KEYWORDS: Antarctica; Data quality control; In situ atmospheric observations; Instrumentation/sensors

1. Introduction

Near-surface air temperature measurements over the Antarctic Plateau (AP) are important both for climate change monitoring and for model validation (e.g., Bracegirdle and Marshall 2012). Because of its remoteness and harsh environment, automatic weather stations (AWSs) are installed on the AP and transmit observed temperature data via satellite (Lazzara et al. 2012). It is, however, difficult to obtain accurate temperatures on the snow-covered regions of Antarctica because most temperature measurements are subject to systematic errors resulting from the heating of the sensor by solar radiation (e.g., Hardy et al. 1998; Arck and Scherer 2001; Georges and Kaser 2002; Huwald et al. 2009; Genthon et al. 2011). In general, radiative heating errors increase with increasing solar radiation and are reduced with increasing ventilation flow. To minimize these errors, an AWS temperature sensor is enclosed in a radiation shield with a forced ventilation system. Because of shortages of power supply to run ventilated shields, however, naturally ventilated (NV) radiation shields are often used in Antarctica instead of force-ventilated (FV) radiation shields. The NV can only reduce the influence of radiative heating and cannot completely eliminate the errors. When ventilation is inadequate to remove the influence of radiative heating, NV temperature measurements result in higher values (hereinafter referred to as radiative error) than the FV measurements.

The magnitude of the radiative error varies considerably depending on the type and surface area of the temperature sensor (Blonquist and Bugbee 2017), the shape and material of the radiation shield, and the surface properties of the ground. Because snow-covered surfaces have a very high albedo, surface-reflected solar radiation entering from below is absorbed in the radiation shield and leads to an increase in radiative error (Richardson et al. 1999). The past studies reported that the errors reached more than 10°C on the snow surface (e.g., Hardy et al. 1998). On the AP, since cloud-free skies dominate with intense incident solar radiation during midnight sun, the errors exceeding 10°C frequently occur when the wind speed is low (Genthon et al. 2011). It is necessary to apply quality control to remove these errors. To minimize the influence of the errors, Genthon et al. (2011) proposed quality control to use only the temperature data with higher wind speeds than a given threshold (4–6 m s^{-1}). However, such filtering results in large data loss because low-wind conditions occur very frequently in austral summer on

Corresponding author: Naoyuki Kurita, nkurita@nagoya-u.jp

DOI: 10.1175/JTECH-D-21-0107.1

the AP. They noted that more than one-half of the data would be filtered out and this approach may bias the observations against calm conditions, making it harder to detect a global warming signal and evaluate reanalysis products on the AP.

Several studies have been proposed to correct for temperature errors induced by radiation forcing (e.g., Anderson and Baumgartner 1998; Arck and Scherer 2001; Nakamura and Mahrt 2005; Mauder et al. 2008). Huwald et al. (2009) reported the robustness of the radiative error-correction model proposed by Nakamura and Mahrt (2005) over a snow-covered site. Their model is based on the similarity regression approach using wind speed and shortwave radiation.

Here we present radiative errors of NV temperature measurements in Dronning Maud Land (DML) on the East Antarctic Plateau. FV measurements from newly installed AWSs are used as a reference to quantify the errors. Similar to Huwald et al. (2009), we apply the regression model to data from AWSs and then quantify the errors in NV measurements in inland DML. The next section presents the instrumentation and AWS observation sites used in this study. The radiative errors at each site and the correction of the errors are discussed in sections 3 and 4, respectively. The general conclusions are summarized in section 5.

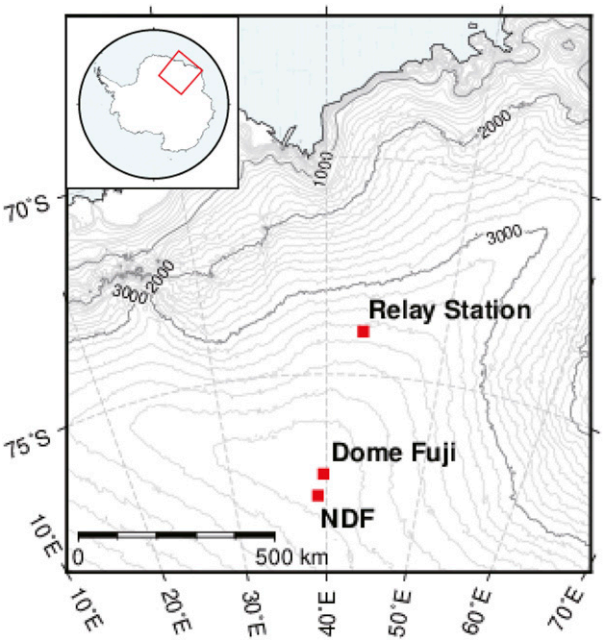

FIG. 1. Elevation map of the east Dronning Maud Land in East Antarctica. Red squares represent the AWS sites at NDF, Dome, and Relay Station, as marked.

2. Data

a. AWSs in inland Dronning Maud Land

In this study, we make use of data from AWSs that were deployed by the Japanese Antarctic Research Expedition (JARE) in inland Dronning Maud Land in the East Antarctica (Fig. 1). In 2018, the JARE installed AWS at two sites, NDF (77.79°S, 39.06°E; 3742 m MSL) in January and Relay Station (74.01°S, 42.98°E; 3354 m MSL) in October. The AWSs measure air temperature and relative humidity with a Vaisala, Inc., Humicap HMP155 at 2.5 ± 0.3 m, wind speed and direction with an R. M. Young Co. anemometer (YG-5108) at ~4 m, and absolute air pressure with a Vaisala Barocap (PTB210) buried at the base of the AWS. Radiation measurements are also conducted using a Kipp and Zonen, Inc., CNR4 radiometer at NDF. An air temperature sensor is enclosed in the mechanically ventilated multiplate (12 plates) shield manufactured by PREDE, Inc. (PRV 100). The airflow of the PRV100 is bottom up with a DC fan at the top of the shield. During polar night, the fan stops running because the fan is powered by solar panels, so the shield is naturally ventilated by wind. In addition to the FV air temperature sensor, an NV sensor (HMP155), housed in a multiplate (14 plates) shield (R. M. Young 41003), is mounted next to the FV sensor at the same levels at NDF (Fig. 2a). Measurements are sampled at 1-min intervals, and 10-min mean values are calculated by the AWS software on the datalogger. These are stored on a memory card and transmitted back via Argos satellite communication.

In addition to the newly installed AWSs by JARE (JARE-AWSs), there are four AWSs (Mizuho, Relay Station, JASE2007, and Dome Fuji) deployed by the University of Wisconsin's Antarctic Meteorological Research and Data Center (AMRDC; the AWS is referred to hereinafter as UW-AWS) (Lazzara et al. 2012). Air temperature is measured at one level (1.5–2.5 m above the surface) by a Weed 1000-Ω platinum resistance thermometer enclosed in a cylindrical radiation shield made of aluminum. This shield was originally designed by the University of Wisconsin–Madison AWS program (Fig. 2b). It protects the sensor from incident solar radiation and allows natural ventilation. The 76.2-mm (3 in.) outside diameter, 1.65-mm-thick (0.065 in.) shield is made from aluminum and has 3M polyester 850 low-emissivity highly reflective (including infrared radiation) tape on the outside. Although the open bottom of the shield does not protect from the surface-reflected solar radiation, the inner black surface (the paint was Krylon ultra flat black paint; manufacturer's part number 104K01602A07) reduces the sensor heating from reflected solar radiation by absorbing the radiation. The large ratio of the shield's surface area to its mass allows the absorbed energy to be dissipated with minimal heating of the sensor under all but very low wind conditions. Additionally, the Weed PRT is covered in the same silver tape to reduce any heating due to reflected radiation from the snow surface, direct radiation during low sun angles, and the thermal IR radiation emitted from the black surface.

This simply designed shield is completely different from the multiplate radiation shield but is commonly used in the Antarctic network of UW-AWSs. Thus, it is valuable to quantify the radiative heating errors of each shield. In this study, we compare the NV temperature observations from two UW-AWSs, Relay Station and Dome Fuji, with the FV temperature observations from the JARE-AWSs, NDF and Relay Station. Relay Station UW-AWS is less than 1 km away from

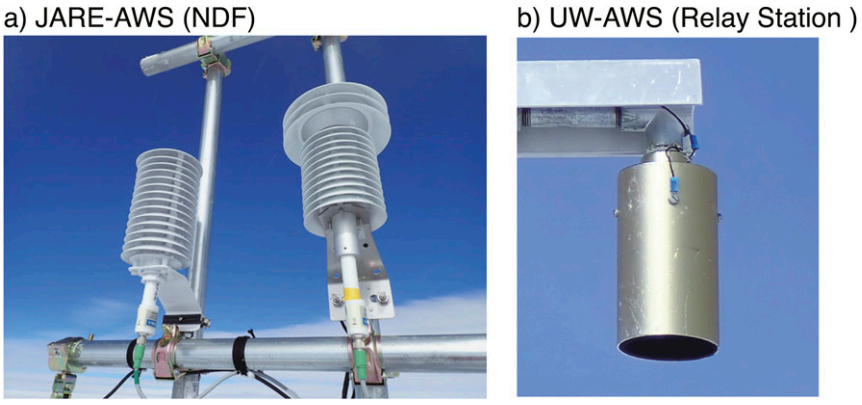

FIG. 2. (a) The naturally ventilated (in the left of the photograph) and mechanically ventilated (on the right) radiation shields of JARE-AWS at NDF. (b) The naturally ventilated radiation shield of UW-AWS at Relay Station.

the location of the JARE-AWS. Dome Fuji UW-AWS is located 60 km northwest of the JARE-AWS, NDF. Since the orography is relatively flat and homogeneous (Fig. 1), comparing the two sensors between NDF JARE-AWS and Dome Fuji UW-AWS is possible if we extract the days when the temperatures at both sites are synchronized. Temperature measurements by the JARE-AWS (HMP155) are based on platinum resistance (PT100), so that the difference of sensors between JARE- and UW-AWS is subtle. The radiative error by a cylindrical radiation shield may be a dominant source of temperature differences.

In this study, we used quality controlled (QC) 10-min mean temperature data of UW-AWSs distributed through the AMRDC website/FTP at the University of Wisconsin (https://amrc.ssec.wisc.edu/data/ and ftp://amrc.ssec.wisc.edu) and soon to be added to its new data repository (https://amrdcdata.ssec.wisc.edu). For the JARE-AWSs, the same QC procedure [see details in Lazzara et al. (2012)] was applied to remove suspicious data that were unlikely to reflect the natural variability. Here we calculated hourly mean data from the QC 10-min mean values and then used hourly data to discuss the radiative errors.

b. *Reanalysis data*

Radiation data are not available at Relay Station. Relay Station is 430 km away from NDF, so it is too far to use the observations at NDF. Here we use the state-of-art reanalysis data instead of observational data. ERA5 is the fifth-generation global atmospheric reanalysis product from the European Centre for Medium-Range Weather Forecasts (ECMWF; Hersbach et al. 2020). ERA5 provides hourly estimates of incoming and reflected shortwave radiation. The horizontal resolution is approximately 31 km. Since cloud-free sky conditions with very low aerosol loading prevail over the AP, we expect that ERA5 shortwave radiation may reasonably match the observations. As expected, the incoming shortwave radiation of ERA5 well reproduced the observed diurnal and seasonal variability from early January to the end of April at NDF (Fig. 3).

3. Analysis of radiative errors in inland Dronning Maud Land

a. *NDF*

Figure 4 shows typical diurnal cycles of air temperature measured from FV and NV sensors during clear sky conditions in midaustral summer at NDF. On 19 January 2018, when wind speeds were less than 4 m s^{-1}, the temperature differences between the FV and the NV sensors clearly reflected a diurnal cycle of solar radiation, which reached the maximum peak (around 8°C) at local noon. On 21 January 2018, when wind speeds exceeded 4 m s^{-1}, the difference did not match the diurnal pattern, and the maximum difference of about 3°C was observed when the wind speed was at the daily minimum. One can notice that the NV measurements showed positive values throughout the day. On the AP in austral summer, the sun never sets over a period of 24 h, and shortwave radiation is always greater than zero. Therefore, the radiative errors were not entirely reduced by the multiplate NV shield, but remained positive throughout the day.

Seasonal variability of temperatures measured by both the FV and NV sensors, wind speed, and reflected shortwave radiation from the early January to the end of June in 2018 are shown in Figs. 5a–d. In this study, we focus on the reflected shortwave radiation rather than incident solar radiation (Fig. 5a). The past study noted that the radiation shields are less protective of reflected solar radiation (e.g., Richardson et al. 1999). In addition, many studies reported that surface-reflected solar radiation has a major impact on the radiative errors (Arck and Scherer 2001; Georges and Kaser 2002; Huwald et al. 2009). In Fig. 5d, the maximum errors of around 8°C appeared until early February and then gradually decreased with reduced reflected shortwave radiation. This seasonal trend suggests that the radiative errors depend not only on the solar irradiance, but also on the zenith angle of the sun. After March 2018, temperature approached the lowest annual temperature and extremely harsh conditions at NDF occasionally affected the operation of the instruments,

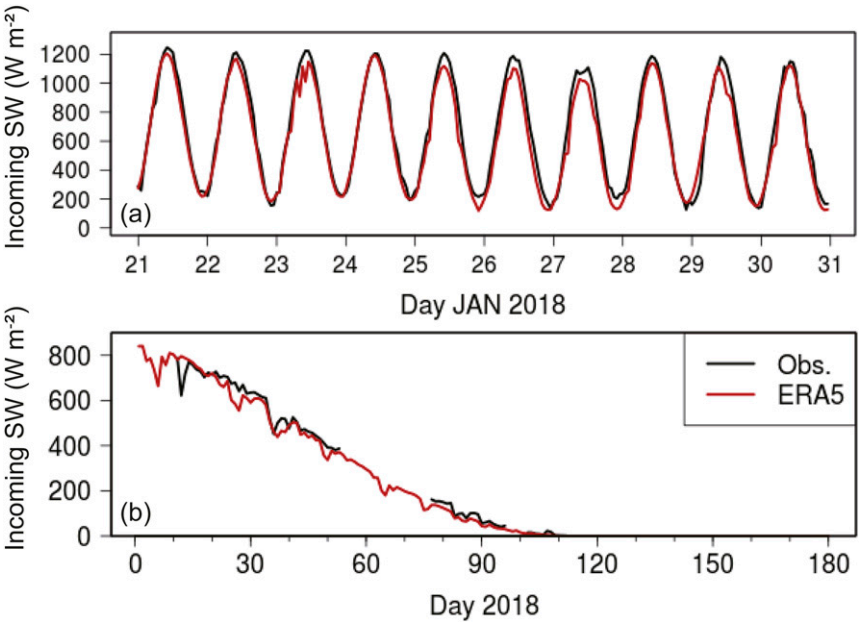

FIG. 3. (a) Hourly incoming (incident + reflected) shortwave radiation of ERA5 (red) and of AWS observation (black) at NDF, 21–30 Jan 2018. (b) Daily mean shortwave radiation of ERA5 (red) and observations (black) at NDF, January–April 2018. The daily mean is calculated when all hourly data are available for that day.

so that the temperature record was not fully continuous. The differences between sensors varied randomly within ±2°C after early March. Although both sensors are naturally ventilated during the polar night, the differences of less than 2°C were well matched with the differences between FV and NV at Dome C (Genthon et al. 2011). Thus, we only

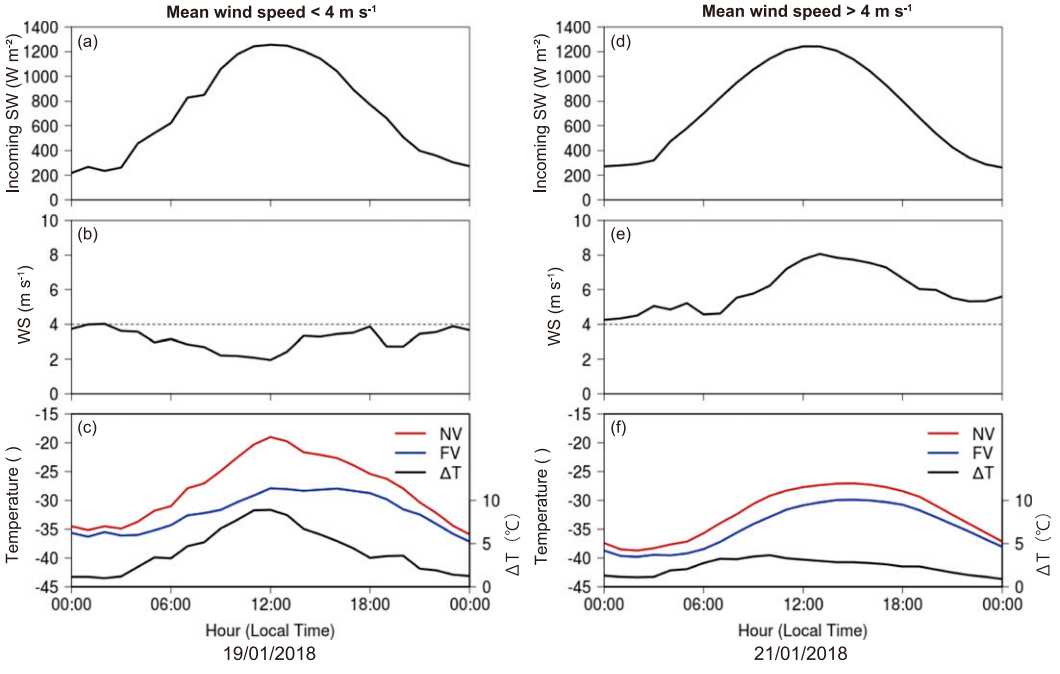

FIG. 4. Diurnal cycles of (a),(d) incoming shortwave radiation, (b),(e) wind speed, and (c),(f) air temperature measured from naturally (red; left axis) and mechanically (blue; left axis) ventilated sensors and the difference of them ΔT (black; right axis) when wind speed (left) was less than 4 m s^{-1} through a day (19 Jan 2018) and (right) exceeded 4 m s^{-1} through a day (21 Jan 2018) at NDF.

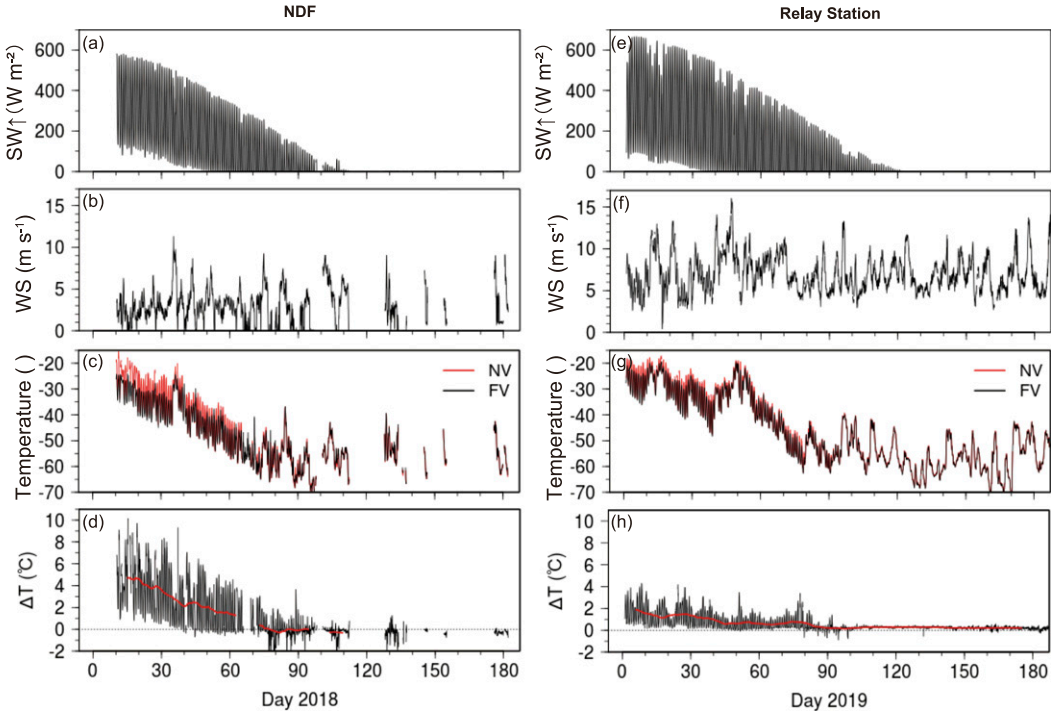

FIG. 5. Seasonal variability of (a),(e) reflected shortwave radiation, (b),(f) wind speed, (c),(g) air temperature measured from naturally (red) and mechanically (blue) ventilated sensors, and (d),(h) the difference of them ΔT (black) with the 10-day moving average (red) from early January to the end of June (left) in 2018 at NDF and (right) in 2019 at Relay Station.

considered the radiative errors greater than 2°C, as previous study has done.

Next, we explored the dependence of the temperature errors on reflected shortwave radiation and wind speed in austral summer (Figs. 6a,b). There is a clear relationship between temperature errors and shortwave radiation. The temperature errors and their spread increase linearly with increasing shortwave radiation. In contrast, the dependence on wind speed shows a decreasing trend. The large spread of errors at low wind speeds nonlinearly decreases to zero with the increase in wind speeds. These features are consistent with the results of previous studies conducted on snow-covered areas (Huwald et al. 2009). However, note that significant temperature errors are seen when winds are above 6 m s^{-1} in midsummer. In previous study at Dome C (Genthon et al. 2011), errors do not persist for winds above 6 m s^{-1}. The mean wind speed (about 2.5 m s^{-1}) in midsummer at NDF is weaker than Dome C, and winds exceeding 6 m s^{-1} do not last long. The occasional strong winds may not be enough for sufficient ventilation of the shield.

b. Relay Station

For comparison, we examined the seasonal variability of radiative errors, wind speed and reflected shortwave radiation at Relay Station (Figs. 5e–h). Figure 5h shows the comparison of air temperature measured by both the NV sensor of UW-AWS and the FV sensor of JARE-AWS from early January to the end of June in 2019. The height of the temperature sensor is not the same between the two AWSs (2.3 m for the UW-AWS, 2.8 m for the JARE-AWS); however, it is minor as the measurements of the two AWSs were almost identical during the polar night. According to Genthon et al. (2010), air is well mixed by turbulence or convection in austral summer on the East Antarctic Plateau. They reported that the nocturnal temperature inversion is weak [1°C (10 m)$^{-1}$]. The radiation error would therefore be a dominant source of temperature difference. Similar to the NDF, the seasonal change of radiative errors showed a gradual decreasing trend with reduced reflected shortwave radiation. However, focusing on the magnitude of radiative errors, we found that the temperature differences are drastically smaller than those measured at NDF. The range of errors from midsummer until polar night was almost half as much as that of NDF, although the seasonal range of shortwave radiation and temperature were approximately the same as at NDF. One of the reasons is the relatively high wind conditions at Relay Station. The mean wind in midsummer (January) was more than 2 times as strong as at NDF (6.8 m s^{-1} for Relay Station; 2.5 m s^{-1} for NDF). Therefore, the relatively higher winds would enhance the ventilation of the shield.

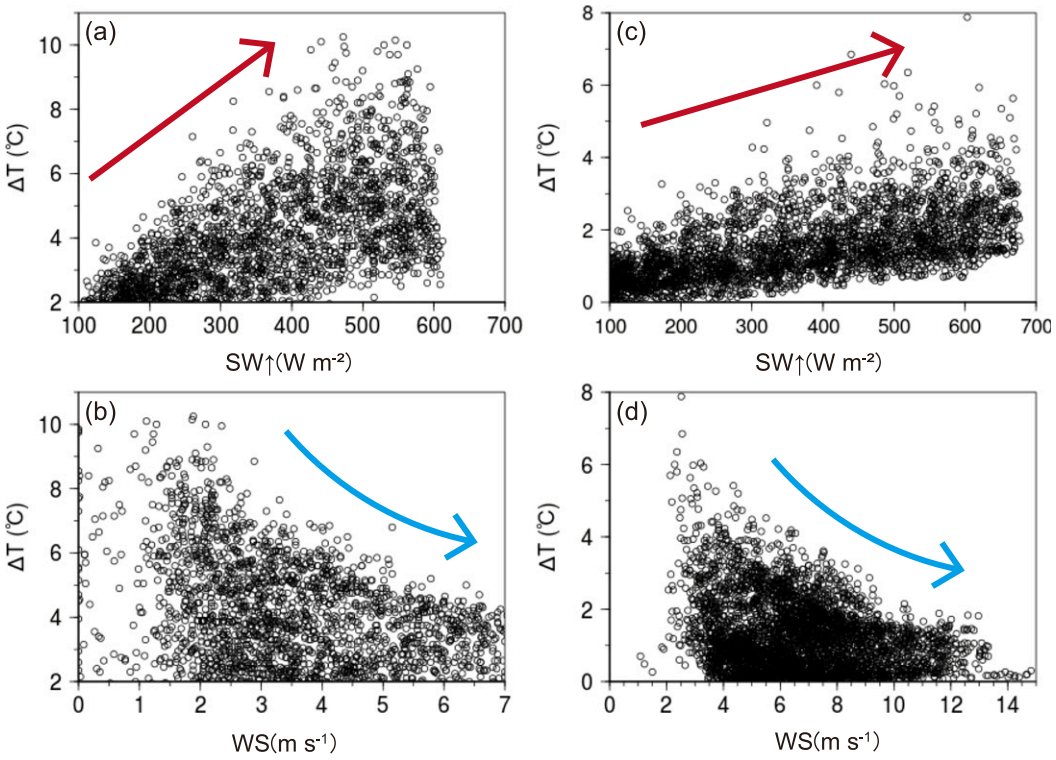

FIG. 6. Radiative errors ΔT vs (a),(c) reflected shortwave radiation and (b),(d) wind speed in austral summer at (left) NDF and (right) Relay Station. The colored arrows give the general trend of the data.

Figures 6c and 6d display the radiative errors as a function of reflected shortwave radiation and wind speed in summer 2019. The general tendency of each variable is similar between NDF and Relay Station. Despite a comparable amount of shortwave radiation at both sites, there are some differences in the wind speed dependency. In Fig. 6d, the spread of radiative errors for low winds below 4 m s^{-1} is clearly lower than that at NDF (Fig. 6b). In addition, the errors for winds above 6 m s^{-1} are reduced to less than half of those at NDF. These indicate that less radiative energy reaches the temperature sensor or that more efficient ventilation cools the temperature sensor. In other words, the NV shield of UW-AWS perform better than the multiplate shield used on the JARE-AWS. Surprisingly, this result contradicts the previous study at Dome C (Genthon et al. 2011), so further investigation is necessary to conclude which radiation shield is better.

c. *Dome Fuji*

To verify the results at Relay Station, we explored the differences of temperature measured by both the NV sensor of Dome Fuji AWS and the FV sensor of NDF AWS. Because Dome Fuji is 60 km apart from NDF, the temperature difference depends not only on the radiative errors, but also on various other factors including offset. The offset between two sites was examined using the temperature when daily mean wind is above 6 m s^{-1} during the polar night. These are unfavorable conditions for the development of a strong temperature inversion, so temperature differences may mainly reflect the systematic bias between the sites. The winter mean temperature from 2018 to 2019 at Dome Fuji was 0.8°C warmer than at NDF. Therefore, we added the offset of Dome Fuji by 0.8°C before comparison with the FV at NDF. Next, we considered the mesoscale temperature fluctuations (González et al. 2021). The occurrence of mesoscale eddies might result in a sharp temperature gradient between NDF and Dome Fuji. To minimize this effect, we extracted only the days when the FV temperature is the same, within 2°C, in both the early morning and the late evening, and reflected shortwave radiation was less than 200 W m^{-2}. We found 46 days in austral summer in both 2018 and 2019.

Figure 7 displays the radiative errors for high reflected shortwave radiation above 500 W m^{-2} as a function of wind speed. To compare the wind speed dependency between the three AWS, the original hourly radiative errors were averaged for bins of wind speed with a range of 2 m s^{-1}. It is clear that the radiative errors at NDF show higher values than at Relay Station and Dome Fuji, independent of wind speed. In addition, the dependence on wind speed at Dome Fuji agrees well with that at Relay Station. From these results, we can say that the simple cylinder-shaped shield used for UW-AWS seems to absorb less radiative energy and/or has a higher ventilation efficiency than the multiplate shield in inland DML.

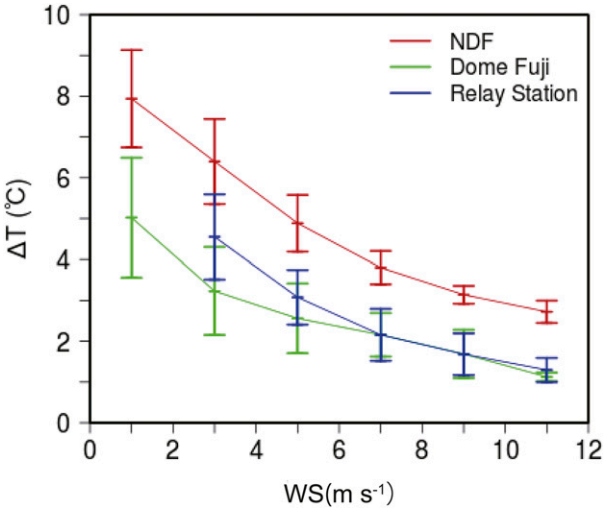

FIG. 7. Bin-averaged radiative errors ΔT for high reflected shortwave radiation above 500 W m^{-2} with respect to wind speed in austral summer at NDF (red), Dome Fuji (green), and Relay Station (blue). Vertical bars indicate standard deviations.

4. Correlation of heating errors

As noted in the previous sections, the radiative errors at each site showed a linear increasing trend with reflected shortwave radiation and a nonlinear decreasing trend with wind speed. These features are consistent with previous studies (e.g., Nakamura and Mahrt 2005; Huwald et al. 2009). Huwald et al. (2009) applied the similarity regression model proposed by Nakamura and Mahrt (2005) to their data and showed the robustness of their model on the snow-covered glacier. This regression model expresses the radiative error as a function of a nondimensional variable: the ratio of the heating by solar radiation to the cooling of natural ventilation. Huwald et al. (2009) noted that usage of reflected shortwave radiation to calculate this variable is more relevant than that of incident shortwave radiation. Here we apply this approach and calculate a nondimensional variable X as follows:

$$X = \frac{\mathrm{SW_{ref}}}{\rho C_p T_{\mathrm{raw}} U},$$

where $\mathrm{SW_{ref}}$ is reflected shortwave radiation, ρ is air density (kg m^{-3}), C_p is specific heat capacity of air (J kg^{-1} K^{-1}), and T_{raw} (K) and U (m s^{-1}) are the measured air temperature and wind speed, respectively. Figure 8a presents a comparison of temperature errors at NDF in austral summer with the nondimensional variable X. We can see a clear linear trend with winds above 2 m s^{-1} (black line), but it curves with increasing radiative errors for all data, including the data with winds less than 2 m s^{-1} (red line). This nonlinear behavior is similar to an earlier study conducted on the snow-covered glacier fields (Huwald et al. 2009), although the coefficients of the regression polynomial here are larger than their study. The robustness of this regression model is shown in Fig. 8d. The NV temperatures corrected by the regression curve with all data (red line) are in good agreement with the FV observations. The reduction of the root-mean-square error (RMSE) reached more than 70%. Thus, this correction procedure can reduce both the mean and RMSE for all data including in conditions of weak wind and intense solar radiation. For Relay Station, the radiative errors change linearly with respect to X because most of the data have wind speeds of greater than 2 m s^{-1} (Fig. 8b). The regression line of Relay Station (blue line) is slightly different than that of NDF with wind speeds above 2 m s^{-1} (black line). The slope of the linear regression line is 7.8 for NDF and 6.1 for Relay Station. The low slope indicates low heating or high cooling efficiency of the radiation shield at Relay Station. This is consistent with our finding that the radiation shield of UW-AWS performs better than the NV shield at NDF. There appears to be a unique regression depending on the sensor/shield combination. To confirm this, we applied the regression line for Relay Station to the data from Dome Fuji. As expected, the radiative errors with wind speeds above 2 m s^{-1} at Dome Fuji are distributed along the regression line for Relay Station (Fig. 8c). The fact that the radiative errors are reduced at all sites after the correction shows the robustness of this regression model to the data in inland DML. The reduction of the RMSE at Relay Station is about the same as at NDF (70%), but that at Dome Fuji is limited. The relatively large RMSE at Dome Fuji reflects the insufficient correction for data with weak wind speeds.

5. Conclusions

Surface air temperatures measured by a naturally ventilated shield in inland Dronning Maud Land showed higher values than those by a mechanically ventilated shield due to solar radiative heating. During the austral summer, cloud-free skies dominated and the sun never sets over a period of 24 h, so radiative heating error showed positive values throughout the summer. Radiative errors were strong functions of reflected solar radiation and wind speed. They increased with increasing reflected shortwave radiation and decreased with increasing wind speed. The hourly mean temperature errors occasionally reached up to 8°C at noon on a sunny day with weak wind conditions at NDF. These features were observed from the measurements not only with the commercially available multiplate radiation shield, but also with the simple cylindrical radiation shield developed by the University of Wisconsin. It is noteworthy that the range of radiative error measured with the simple cylindrical shield was much narrower that with the standard multiplate shield. This suggests that the radiation shield developed by the UW performs better than the multiplate shield. This is unexpected, but it may be related to the persistent clear sky with weak wind conditions throughout the summer. Hoar-frost tends to develop under such weather conditions and accumulates in the gaps between the plates of the multiplate shield. The accumulation of hoarfrost on the shield would largely reduce the ventilation efficiency, which could then lead to radiative heating.

A majority of meteorological observations have been conducted by AWS network over the past 30 years on the

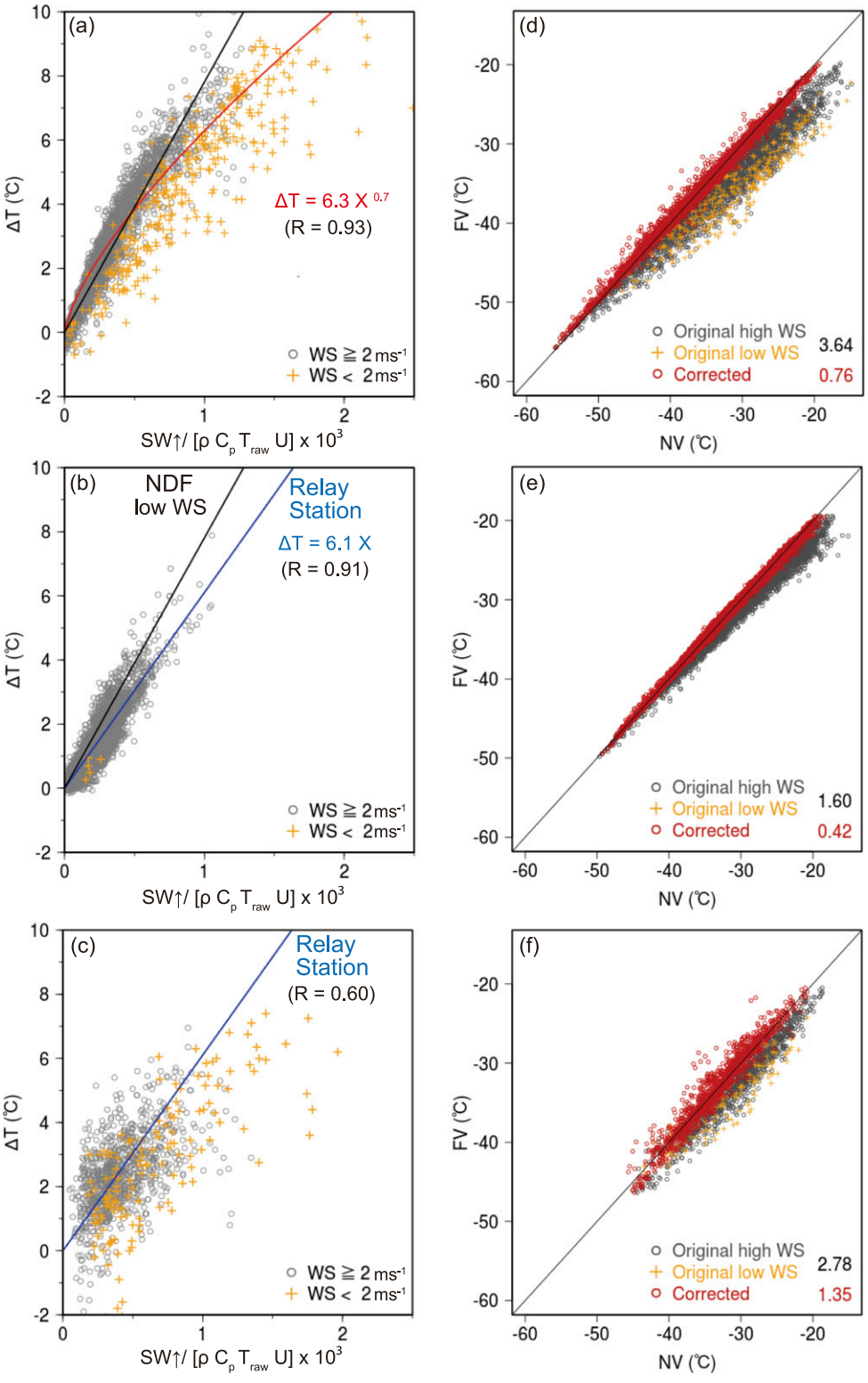

FIG. 8. Radiative errors ΔT as a function of the nondimensional variable in winds below 2 m s^{-1} (orange crosses) and in winds more than 2 m s^{-1} (gray circles) in austral summer at (a) NDF, (b) Relay Station, and (c) Dome Fuji. For better display, the nondimensional variable is multiplied by a factor of 10^3. The red line represents the regression curve with all plots including both weak (lower than 2 m s^{-1} of wind speed) and strong (higher than 2 m s^{-1} of wind speed) winds at NDF in (a). The black line in (a) and (b) is the regression

←
line with winds more than 2 m^{-1} at NDF. The blue line in (b) and (c) is the same as the black line but for Relay Station. Also shown is temperature measured from force-ventilated (FV) sensors vs original (black circles and orange crosses) and corrected temperature (red) measured from naturally ventilated (NV) sensors in austral summer at (d) NDF, (e) Relay Station, and (f) Dome Fuji. The black line represents 1:1. The root-mean-square errors between FV temperature and original (black) or corrected (red) NV temperature are also shown.

Antarctic Plateau. Naturally ventilated shields are commonly used for temperature measurements on AWSs. Removing the radiative errors from AWS data is essential to examine Antarctic climate change and to validate the reanalysis data and meteorological models. Therefore, it is crucial to quantify the radiative heating errors in temperature observations made by UW-AWS widely installed over Antarctica. In this study, we applied an existing correction model based on applying a similarity regression approach (Nakamura and Mahrt 2005) to AWS data, which could considerably reduce both the mean and root-mean-square error of the radiative error after the correction. At Relay Station, the reduction of RMSE for the errors of the UW-AWS reached more than 70%. The robustness of the correction model indicates that we can use the corrected temperature data instead of a quality control method to remove radiative errors during weak wind conditions. In inland DML, the UW-AWSs were installed in the mid-1990s and have since observed air temperature and wind speed at Mizuho, Relay Station, JASE2007, and Dome Fuji. The fact that the regression line of Relay Station could apply to the data from Dome Fuji implies that the coefficients of our regression model may be applicable to other two AWSs equipped with the same radiation shield. In addition, ERA5 reflected shortwave radiation reanalysis data cover the whole observation period. Thus, reducing the radiative errors can increase the validity of temperature data in inland DML on the East Antarctic Plateau.

Acknowledgments. This study was supported by National Institute of Polar Research (NIPR) through Project Research KP-302. This study was conducted as parts of two Scientific Programs under the Japanese Antarctic Research Expedition (JARE), which are titled "Mechanism of variation in surface condition of the ice sheet and heat and moisture budget in east Antarctica" (project AP0911) and "Antarctic paleoenvironmental reconstructions for unraveling the Earth system variations" (project AJ0903). It was supported by the National Institute of Polar Research (NIPR) under MEXT. This work was supported by JSPS KAKENHI Grant 18K19851. The UW-AWS program is funded by U.S. National Science Foundation Grant 1924730.

Data availability statement. AWS data conducted by JARE will be publicly available through the Arctic and Antarctic Data Archive System (AADS) website at the National Institute of Polar Research (https://ads.nipr.ac.jp/real-time-monitors). The other AWS data can be accessed through the Antarctic Meteorological Research and Data Center (AMRDC) website and FTP site at the University of Wisconsin (https://amrc.ssec.wisc.edu/data/ and ftp://amrc.ssec.wisc.edu). Soon, these data will be placed in the AMRDC repository (https://amrdcdata.ssec.wisc.edu).

REFERENCES

Anderson, S. P., and M. F. Baumgartner, 1998: Radiative heating errors in naturally ventilated air temperature measurements made from buoys. *J. Atmos. Oceanic Technol.*, **15**, 157–173, https://doi.org/10.1175/1520-0426(1998)015<0157:RHEINV>2.0.CO;2.

Arck, M., and D. Scherer, 2001: A physically based method for correcting temperature data measured by naturally ventilated sensors over snow. *J. Glaciol.*, **47**, 665–670, https://doi.org/10.3189/172756501781831774.

Blonquist, M., and B. Bugbee, 2017: Instruments and approaches for accurate measurement of air temperature. *Agroclimatology*, J. Hatfield, Ed., American Society of Agronomy, 51–72.

Bracegirdle, T., and G. Marshall, 2012: The reliability of Antarctic tropospheric pressure and temperature in the latest global reanalyses. *J. Climate*, **25**, 7138–7146, https://doi.org/10.1175/JCLI-D-11-00685.1.

Genthon, C., M. S. Town, D. Six, V. Favier, S. Argentini, and A. Pellegrini, 2010: Meteorological atmospheric boundary layer measurements and ECMWF analyses during summer at Dome C, Antarctica. *J. Geophys. Res.*, **115**, D05104, https://doi.org/10.1029/2009JD012741.

——, D. Six, V. Favier, M. Lazzara, and L. Keller, 2011: Atmospheric temperature measurement biases on the Antarctic Plateau. *J. Atmos. Oceanic Technol.*, **28**, 1598–1605, https://doi.org/10.1175/JTECH-D-11-00095.1.

Georges, C., and G. Kaser, 2002: Ventilated and unventilated air temperature measurements for glacier-climate studies on a tropical high mountain site. *J. Geophys. Res.*, **107**, 4775, https://doi.org/10.1029/2002JD002503.

González, S., F. Vasallo, P. Sanz, A. Quesada, and A. Justel, 2021: Characterization of the summer surface mesoscale dynamics at Dome F, Antarctica. *Atmos. Res.*, **259**, 105699, https://doi.org/10.1016/j.atmosres.2021.105699.

Hardy, D. R., M. Vuille, C. Braun, F. Keimig, and R. S. Bradkey, 1998: Annual and daily meteorological cycles at high altitude on a tropical mountain. *Bull. Amer. Meteor. Soc.*, **79**, 1899–1913, https://doi.org/10.1175/1520-0477(1998)079<1899:AADMCA>2.0.CO;2.

Hersbach, H., and Coauthors, 2020: The ERA5 global reanalysis. *Quart. J. Roy. Meteor. Soc.*, **146**, 1999–2049, https://doi.org/10.1002/qj.3803.

Huwald, H., C. W. Higgins, M.-O. Boldi, E. Bou-Zeid, M. Lehning, and M. B. Parlange, 2009: Albedo effect on radiative errors in air temperature measurements. *Water Resour. Res.*, **45**, W08431, https://doi.org/10.1029/2008WR007600.

Lazzara, M. A., G. A. Weidner, L. M. Keller, J. E. Thom, and J. J. Cassano, 2012: Antarctic automatic weather station

program: 30 years of polar observation. *Bull. Amer. Meteor. Soc.*, **93**, 1519–1537, https://doi.org/10.1175/BAMS-D-11-00015.1.

Mauder, M., R. L. Desjardins, and R. Haarlem, 2008: Errors of naturally ventilated air temperature measurements in a spatial observation network. *J. Atmos. Oceanic Technol.*, **25**, 2145–2151, https://doi.org/10.1175/2008JTECHA1046.1.

Nakamura, R., and L. Mahrt, 2005: Air temperature measurement errors in naturally ventilated radiation shields. *J. Atmos. Oceanic Technol.*, **22**, 1046–1058, https://doi.org/10.1175/JTECH1762.1.

Richardson, S. J., F. V. Brock, S. R. Semmer, and C. Jirak, 1999: Minimizing errors associated with multiplate radiation shields. *J. Atmos. Oceanic Technol.*, **16**, 1862–1872, https://doi.org/10.1175/1520-0426(1999)016<1862:MEAWMR>2.0.CO;2.